0026-895X/95/050923-11$3.00/0

MOLECULAR PHARMACOLOGY, 47:923–933 (1995).

Vasoactive Intestinal Peptide Elevates Pinealocyte Intracellular Calcium Concentrations by Enhancing Influx: Evidence for Involvement of a Cyclic GMP-Dependent Mechanism

NICOLAS C. SCHAAD,[1] JIRI VANECEK, IGNACIO R. RODRIGUEZ, DAVID C. KLEIN,[1] LYNNE HOLTZCLAW, and JAMES T. RUSSELL

Section on Neuroendocrinology, Laboratory of Developmental Neurobiology (N.C.S., D.C.K.), and Section on Neuronal Secretory Systems, Laboratory of Cellular and Molecular Neurophysiology (L.H., J.T.R.), National Institute of Child Health and Human Development, and Laboratory of Retinal Cell and Molecular Biology, National Eye Institute (I.R.R.), National Institutes of Health, Bethesda, Maryland 20892, and Institute of Physiology, Czech Academy of Sciences, Prague, The Czech Republic (J.V.)

Received October 19, 1994; Accepted February 16, 1995

SUMMARY

Vasoactive intestinal peptide (VIP) receptor density is high in the pineal gland, which receives VIP innervation and responds to VIP with a relatively small increase in cAMP and cGMP levels. In the present study, we show that VIP (5–200 nM) treatment increased the intracellular calcium concentration ($[Ca^{2+}]_i$) in 64% of isolated individual pinealocytes; in comparison, norepinephrine (NE) elevated $[Ca^{2+}]_i$ in 93% of the cells and produced more robust responses. Analysis of the role of second messengers indicated that $[Ca^{2+}]_i$ was strongly elevated by cGMP analogs, but not by cAMP analogs. The nitric oxide-releasing agent *S*-nitro-*N*-acetylpenicillamine and 2,2-diethyl-1-nitroxyhydrazine also elevated $[Ca^{2+}]_i$. Investigation of the mechanisms revealed that responses to VIP or 8-bromo-cGMP involved Ca^{2+} influx, as did the plateau component of the response to NE; the large rapid component of the response to NE, however, appeared to reflect release from intracellular stores. Pharmacological studies indicated that the VIP-induced Ca^{2+} influx was mediated by a retinal rod-type cyclic nucleotide-gated cation channel, expression of which was confirmed by reverse transcription-polymerase chain reaction analysis. These observations indicate that fundamentally different mechanisms generate the responses to NE and VIP. The dominant effect of VIP causing transient elevation of $[Ca^{2+}]_i$ appears to be through cGMP gating a *l-cis*-diltiazem-sensitive rod-type cyclic nucleotide-gated cation channel. In contrast, the dominant effect of NE on $[Ca^{2+}]_i$ is due to enhanced Ca^{2+} release from intracellular stores; the plateau component is due to influx through a *l-cis*-diltiazem-insensitive channel.

The pineal gland has one of the highest densities of VIP receptors in the mammalian brain (1). This tissue receives VIP innervation (2) and is responsive to VIP (3–7). However, some pineal responses to VIP are smaller than those elicited by NE, which is generally considered to be the primary regulator of pineal function (8). For example, whereas both agents elevate pineal cAMP and cGMP levels, the effects of NE are ~10-fold greater than those of VIP; smaller differences exist between the effects of VIP and NE on stimulation of NAT and melatonin production (9–12).

An important element in NE signal transduction in the pineal gland is a sustained, α-adrenergic receptor-mediated elevation of $[Ca^{2+}]_i$ (10, 13, 14). This is essential for NE to generate maximal increases in the accumulation of cyclic nucleotides (9, 11). In addition, elevation of $[Ca^{2+}]_i$ potentiates the effects of cAMP on K^+ efflux and on NAT activity and may contribute to the relatively larger stimulation of NAT activity by NE (6, 7, 12, 15).

A plausible reason why pinealocyte responses to VIP are smaller than those to NE is that VIP might not elevate $[Ca^{2+}]_i$. This would explain why $[Ca^{2+}]_i$-elevating agents potently increase the effects of VIP on cyclic nucleotide levels (6, 7). The effects of VIP on pinealocyte $[Ca^{2+}]_i$ have not been studied, although VIP does elevate $[Ca^{2+}]_i$ in other cells

This work was done while N.C.S. was a Visiting Fellow and Special Volunteer in the Section on Neuroendocrinology, supported by a grant from the Fond National Suisse de la Recherche Scientifique, and while J.V. was a Visiting Scientist in the Section on Neuroendocrinology, Laboratory of Developmental Neurobiology, National Institute of Child Health and Human Development, National Institutes of Health.

[1] Current address: Division de Psychopharmacologic Clinique, Clinique Psychiatrique de Bel-Air, 1225 Chêne-Bourg, Switzerland.

ABBREVIATIONS: VIP, vasoactive intestinal peptide; NE, norepinephrine; $[Ca^{2+}]_i$, intracellular free Ca^{2+} concentration; $[Ca^{2+}]_o$, extracellular Ca^{2+} concentration; CNG, cyclic nucleotide-gated; DB-cAMP, N^6,2′-*O*-dibutyryl-cAMP; DB-cGMP, N^6,2′-*O*-dibutyryl-cGMP; 8-Br-cAMP, 8-bromo-cAMP; 8-Br-cGMP, 8-bromo-cGMP; SNAP, *S*-nitroso-*N*-acetylpenicillamine; EBSS, Eagle's basal salt solution; AM, acetoxymethyl ester; DMEM, Dulbecco's modified Eagle's medium; NAT, *N*-acetyltransferase; bp, base pair(s); NO, nitric oxide; HEPES, 4-(2-hydroxyethyl)-1-piperazineethanesulfonic acid; PCR, polymerase chain reaction; RT, reverse transcription.

(16–19). To examine the effects of VIP on pinealocyte $[Ca^{2+}]_i$, we have measured fura-2 fluorescence changes in single cells and found that VIP elevates $[Ca^{2+}]_i$ in 64% of the pinealocytes analyzed, apparently via cGMP-dependent stimulation of influx through a rod-type CNG cation channel.

Materials and Methods

Pineal cell culture. A detailed description of pineal cell isolation and culture has been published previously (13). Briefly, pineal glands were isolated from female Sprague-Dawley rats (200–250 g, 20–40 pineal glands/preparation), placed in ice-cold phosphate-buffered saline, and gently disrupted using a pair of forceps. The tissue pieces were then placed in EBSS containing papain (20 units/ml). The EBSS contained, in addition, 0.5 mM EDTA, 1.0 mM L-cysteine, 0.1 mg/ml DNase, 26.2 mM $NaHCO_3$, and 33.3 mM glucose. After an incubation period of 50 min at 37°, the glands were triturated with a pipette, incubated for an additional 10 min, and then triturated again. The suspension was centrifuged (800 × *g* for 5 min at 4°) and cells were resuspended in EBSS containing bovine serum albumin (10 mg/ml) and trypsin inhibitor (10 mg/ml). Individual cells were separated from cell clumps and tissue debris by centrifugation (800 × *g* for 5 min at 4°) through a layer of albumin (10 mg/ml) in EBSS. Cells in the pellet were resuspended in DMEM (supplemented with 10% fetal calf serum), plated on Peptite 2000-coated, number 1, glass coverslips at a density of 10^5/coverslip, and allowed to adhere for 3 hr in the incubator. A 2.0-ml volume of DMEM (containing 10% fetal calf serum) was then added to the coverslips in 35-mm culture dishes, and cells were maintained for 24–48 hr before $[Ca^{2+}]_i$ measurements.

$[Ca^{2+}]_i$ measurements. Cells on coverslips were loaded with fura-2/AM (2 μM), as described previously (13), in DMEM without phenol red (containing 20 mM HEPES and 10% fetal calf serum) at 37° for 10 min, placed in a Leiden coverslip chamber mounted on the microscope stage, and perfused with the same solution at a rate of 1.5 ml/min during experiments. Cells were maintained at 37° throughout the experiments. Drug treatment was accomplished using the "sewer pipe" technique, by changing to perfusion medium containing appropriate concentrations of the drug. $[Ca^{2+}]_i$ measurements were carried out as described previously (13, 20, 21). Briefly, fura-2 fluorescence was observed with an inverted microscope on a vertical optical bench, using a Nikon 40×/1.3 NA CF Fluor DL objective lens. The cells were illuminated with a mercury arc lamp (Oriel Optics), with quartz collector lenses. A shutter (Uniblitz) and a wheel (Lambda-10; Sutter Instruments) containing bandpass filters were mounted in the light path. The computer controlled both the shutter and the filter wheel, such that the cells were alternately illuminated with 340- and 380-nm excitation beams (495 nm for fluo-3). Fluorescence images were acquired through a microchannel plate intensifier (model KS-1380; Videoscope International, Washington DC), with a charge-coupled device camera (Videoscope International). Images were digitized and averaged (two frames at each wavelength) with a Trapix 55/4256 image processor (Recognition Concepts, Incline Village, NV). The time interval between image pairs was varied depending on the required temporal resolution (up to 210 msec/pair). After all image pairs were collected and stored, ratio images were generated on a pixel-by-pixel basis after subtraction of appropriate blanks. The average pixel values in the ratio image were measured on a frame-by-frame basis for each cell in the field of view, to obtain the average ratio as a function of time. The fluorescence ratio data were converted to calcium concentrations from a calibration curve constructed according to the methods of Refs. 22 and 23; the details of this calibration procedure have already been described (20). Data in graphs represent $[Ca^{2+}]_i$ values in single cells (calculated in this manner) plotted versus time. The resting $[Ca^{2+}]_i$ was estimated to be 72.6 ± 0.8 nM (mean ± standard error) in 500 cells, and the values ranged from 36.4 nM to 162.3 nM. Data in tables represent $[Ca^{2+}]_i$ responses calculated after subtraction of basal $[Ca^{2+}]_i$ values, on a cell-by-cell basis, before averaging. Basal values for each cell were calculated by averaging the individual data points collected before agonist addition.

RNA extraction, cDNA synthesis, and PCR. Total RNA was isolated from groups of five rat pineal glands, from retinae, or from cerebella, using a single-step protocol (24) with RNAsol B (Biotecx Laboratories, Houston, TX). One microgram of total RNA was reverse transcribed to cDNA in 50 μl using a kit (Promega), according to the manufacturer's protocol. The CNG calcium channel cDNA was amplified by PCR, using a Perkin-Elmer thermocycler, in Tris buffer, pH 9.2, containing 1.5 mM $MgCl_2$, 25 mM KCl, 50 μM deoxynucleoside triphosphates, 0.5 unit/50 μl PerfectMatch DNA polymerase enhancer (Stratagene, Zurich, Switzerland), 1.25 unit/50 μl AmpliTaq DNA polymerase, and 25 pmol/50 μl primers. The primers used, GTACGAACAAGGACAGGTTAC (positions 637–657) and TGTTGGTCCACAGGTAGTCAA (positions 1321–1301), were selected based on the sequence of the human CNG calcium channel (25). The PCR product was amplified by 40 cycles of denaturation at 94° for 1 min, annealing at 55° for 1.5 min, and extension at 72° for 2 min. PCR products were resolved on 4–20% polyacrylamide gels (Novex, San Diego, CA) and stained with ethidium bromide.

Sequence analysis of PCR products. PCR product bands were identified using ethidium bromide (see Fig. 8), and sections of gel containing bands of interest were removed. Product was extracted from these bands and reamplified using the primers described above. DNA from the reamplifed products was prepared for sequencing using a Wizard PCR Preps DNA purification kit purchased from Promega Corp. (Madison, WI). The purified products were sequenced using the PRISM DyeDeoxy Terminator cycle sequencing kit (Applied Biosystems, Foster City, CA), following the manufacturer's protocol. Typically, 0.5 pmol of template and 3 pmol of primer were used in each sequencing reaction. The sequencing reaction products were purified using Select-D G-50 columns (5 Prime-3 Prime, Boulder, CO) and dried. Each sample was then dissolved in 5 μl of formamide and 1 μl of 50 mM EDTA, heated, and loaded in a model 370A automated fluorescent sequencer (Applied Biosystems). Sequence comparison analysis was performed using the following programs from the Genetics Computer Group Sequence Analysis Software Package (26): FASTA, BESTFIT, and PILEUP.

Materials. The following compounds were purchased or donated: ω-conotoxin (Bachem, Torrence, CA); DB-cGMP, 8-Br-cGMP, 8-Br-cAMP, DB-cAMP, nicardipine, D-600 (methoxyverapamil), and ascorbic acid (Sigma Chemical Co., St. Louis, MO); SNAP, isoproterenol, and prazosin (Research Biochemicals, Natick, MA); *l-cis*-diltiazem (Dr. King Wai Yau, Johns Hopkins School of Medicine, Baltimore, MD); and 2,2-diethyl-1-nitroxyhydrazine (Dr. Tambra Duna, National Cancer Institute, Bethesda, MD). The sources of all other chemicals used have been reported (13).

Statistics. Student's *t* test was used for statistical analysis (27). Statistical analysis was performed on data from all of the cells analyzed on different coverslips that had been treated identically. Typically, each coverslip in a treatment group was prepared on a different day and results were pooled.

Results

Effects of VIP and NE. VIP (0.1 μM) treatment increased $[Ca^{2+}]_i$ in 64% of the pinealocytes on 19 coverslips (number of cells analyzed, 387). Examples of typical patterns of responses to VIP and NE appear in Fig. 1. The VIP response profiles were heterogeneous. In nearly all VIP-responsive cells, $[Ca^{2+}]_i$ tended to return to base-line levels during VIP treatment (Fig. 1), as indicated by the $[Ca^{2+}]_i$ value 90 sec after the beginning of VIP application (Tables 1 and 2). The peak amplitude of the response increased with increasing VIP doses within a concentration range of 5–200 nM (Table

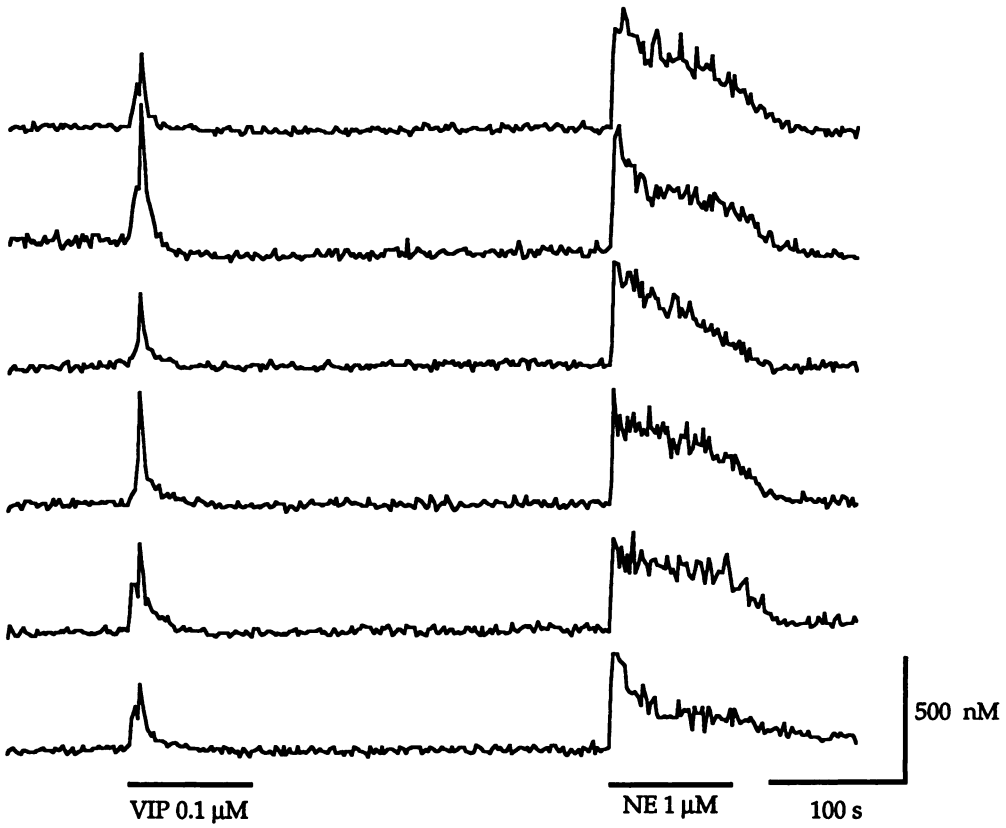

Fig. 1. Effect of VIP on $[Ca^{2+}]_i$ in pinealocytes. Pinealocytes were plated as described in Materials and Methods, loaded with fura-2/AM, and perfused at the rate of 1.5 ml/min at 37° for at least 10 min before the beginning of the recording (time 0). The cells were exposed to VIP followed by NE (*black bars*). Six of 52 cells from one experiment are shown, with an offset on the *ordinate* for clarity.

TABLE 1

Concentration-response analysis of the effects of VIP on pinealocyte $[Ca^{2+}]_i$

This is a summary of results obtained using three preparation of cells, samples of which appear in Fig. 1. Data are presented as the mean ± standard error. *n*, number of cells analyzed.

VIP	$[Ca^{2+}]_i$ response[a]		Integrated response[b]	*n*
	Peak[c]	90 sec[d]		
nM	nM		μM·sec	
1	36 ± 8	20 ± 7.7	2.2 ± 0.5	15
5	50 ± 6	31 ± 4.0	3.0 ± 0.4	15
10	56 ± 7	23 ± 3	2.9 ± 0.4	20
50	63 ± 9	28 ± 6.6	3.8 ± 0.6	31
100	91 ± 5	38 ± 4.0	5.5 ± 0.6	58
200	127 ± 8	23 ± 2.8	7.1 ± 0.5	183

[a] Response values have had pretreatment values subtracted on a cell-by-cell basis.
[b] The integrated response reflects the response during the first 3 min of treatment.
[c] In all cases peak responses occurred during the first 10 sec of treatment.
[d] Values are $[Ca^{2+}]_i$ at 90 sec after initiation of treatment, which provides a measure of the response during the plateau phase.

TABLE 2

Comparative analysis of the effect of selected agonists on pinealocyte $[Ca^{2+}]_i$

This is a summary of the results of a series of experiments, samples of which appear in Figs. 1, 2, and 3. Data are presented as the mean ± standard error. *n*, number of cells analyzed.

Agent	$[Ca^{2+}]_i$ response[a]		Integrated response[b]	*n*
	Peak[c]	90 sec[d]		
	nM		μM·sec	
VIP (0.1 μM)	131 ± 5	19 ± 4	9.5 ± 0.6	129
NE (1 μM)	288 ± 8	105 ± 4	21.9 ± 0.6	281
8-Br-cGMP (1 mM)	100 ± 6	19 ± 2	7.8 ± 0.3	204
SNAP (1 mM)	68 ± 4	35 ± 3	6.2 ± 0.5	222
DB-cGMP (1 mM)	78 ± 8	7 ± 3	5.3 ± 0.6	111

[a] Response values have had pretreatment values subtracted on a cell-by-cell basis.
[b] The integrated response reflects the response during the first 3 min of treatment.
[c] In all cases peak responses occurred during the first 10 sec of treatment.
[d] Values are $[Ca^{2+}]_i$ at 90 sec after initiation of treatment, which provides a measure of the response during the plateau phase.

1). The number of cells responding to VIP also increased over the concentration range tested (data not shown).

The $[Ca^{2+}]_i$ responses of pinealocytes to NE and VIP were compared. NE elevated $[Ca^{2+}]_i$ in a greater percentage of cells (93% of 281 cells) and typically generated an initial spike response followed by a plateau (Fig. 1; Table 2), in agreement with reports in the literature (13, 14). The $[Ca^{2+}]_i$ response to VIP was approximately 50% smaller than the response to NE, as indicated by the peak response and the integrated response measured during the first 3 min of treatment (Tables 2 and 3). In addition, analysis of the response to these agonists 90 sec after treatment indicated that the NE response (37.8 ± 1.4% of the peak NE response) was several-fold greater than the VIP response (8.3 ± 0.6% of the peak VIP response). This analysis emphasizes the fundamental differences in the response profiles of the two agonists, i.e., the response to VIP is transient, whereas the NE response has a peak followed by a plateau as long as agonist is present (Fig. 1).

Studies with cyclic nucleotide protagonists. cAMP is thought to mediate VIP-induced elevation of $[Ca^{2+}]_i$ in other cells (16–18, 28). In our studies, however, the cAMP protagonist 8-Br-cAMP (1 mM) did not increase $[Ca^{2+}]_i$ in any of 48 pinealocytes on three coverslips (Fig. 2D). This agrees with observations on pinealocytes in suspension (11). Similarly,

TABLE 3

Comparative analysis of the effects of selected agonists on $[Ca^{2+}]_i$ in pinealocytes in low-Ca^{2+} (5 μM) and normal-Ca^{2+} (1.5 mM) medium.

This is a summary of the results of a series of experiments, examples of which appear in Fig. 5. Cells were tested first in low-Ca^{2+} medium and then in normal-Ca^{2+} medium. Data are presented as the mean ± standard error. *n*, number of cells analyzed.

Agent	$[Ca^{2+}]_o$	$[Ca^{2+}]_i$ response[a]		Integrated response[b]	*n*
		Peak[c]	90 sec[d]		
		nM		μM·sec	
VIP (0.1 μM)	5 μM	18.5 ± 3.5	6.1 ± 1.50	0.8 ± 0.10	106
	1.5 mM	123.5 ± 2.8	11.2 ± 0.60	11.8 ± 0.10	106
NE (1 μM)	5 μM	222.6 ± 7.1	28.3 ± 3.80	6.8 ± 0.43	104
	1.5 mM	265.7 ± 4.9	135.4 ± 4.00	18.9 ± 0.4	104
8-Br-cGMP (1 mM)	5 μM	10.8 ± 0.8	0.1 ± 1.00	0.1 ± 0.05	51
	15 mM	109.2 ± 3.0	17.3 ± 4.80	6.9 ± 0.70	51
SNAP (1 mM)	5 μM	12.3 ± 2.8	5.2 ± 0.04	0.6 ± 0.05	39
	1.5 mM	66.4 ± 3.5	32.3 ± 6.10	5.8 ± 0.60	39

[a] Response values have had pretreatment values subtracted on a cell-by-cell basis.
[b] The integrated response reflects the response during the first 3 min of treatment.
[c] In all cases peak responses occurred during the first 10 sec of treatment.
[d] Values are $[Ca^{2+}]_i$ at 90 sec after initiation of treatment, which provides a measure of the response during the plateau phase.

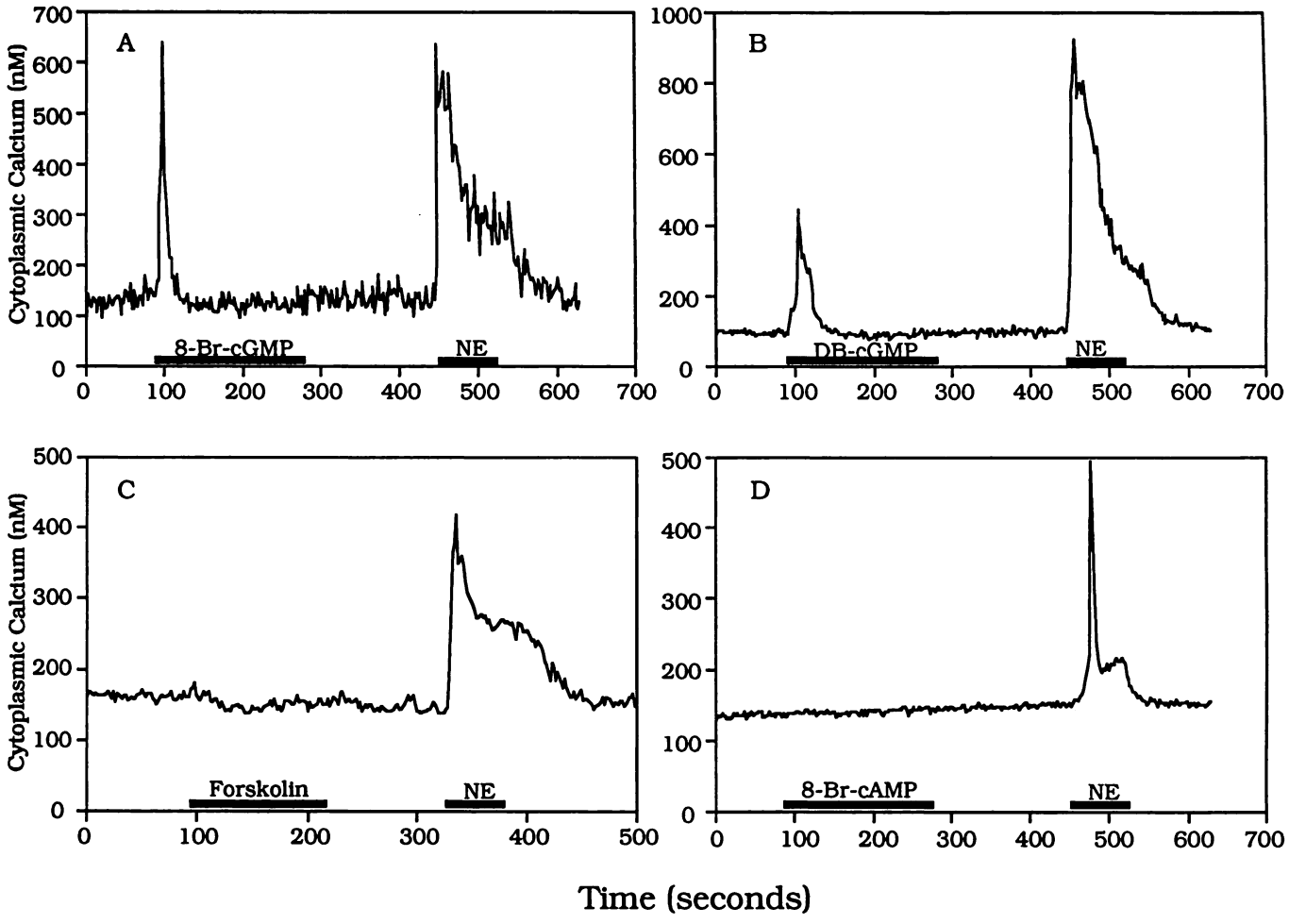

Fig. 2. Effects of cAMP and cGMP protagonists on $[Ca^{2+}]_i$ in pinealocytes. Pinealocytes were plated as described in Materials and Methods, loaded with fura-2/AM, and perfused at the rate of 1.5 ml/min at 37° for at least 300 sec before the beginning of the recording (time 0). Treatment was initiated as indicated (*bars*). Typical results are presented. A, Effect of 8-Br-cGMP. 8-Br-cGMP (1 mM) increased resting $[Ca^{2+}]_i$ in 204 of 267 cells on six coverslips. B, Effect of DB-cGMP. DB-cGMP (1 mM) increased resting $[Ca^{2+}]_i$ in 111 of 159 cells on four coverslips. C, Effect of forskolin. Forskolin (100 μM) did not increase $[Ca^{2+}]_i$ in cells on two coverslips (26 cells). D, Effect of 8-Br-cAMP. 8-Br-cAMP (1 mM) did not increase $[Ca^{2+}]_i$ on three coverslips (48 cells). A quantitative summary of experiments represented by A and B appears in Table 2.

forskolin (100 μM) treatment failed to increase $[Ca^{2+}]_i$ in 26 cells on two coverslips (Fig. 2C). Selective β_1-adrenergic stimulation (50 nM isoproterenol plus 1 μM prazosin), which increases pinealocyte cAMP levels (8), also failed to elevate $[Ca^{2+}]_i$ in 86 cells analyzed (six coverslips) (data not shown), in agreement with previous observations (11).

In contrast to the ineffectiveness of cAMP analogs, two cGMP analogs elevated $[Ca^{2+}]_i$. 8-Br-cGMP treatment (1 mM) increased $[Ca^{2+}]_i$ in 76.5% of 267 cells on 12 coverslips (Fig. 2A; Tables 2 and 3). The response profile varied on a cell-to-cell basis; some cells that were nonresponsive to 8-Br-cGMP responded to NE. The responses to 1 mM and 0.1 mM 8-Br-cGMP were similar; a 10 μM concentration was generally ineffective (data not shown). DB-cGMP treatment increased $[Ca^{2+}]_i$ in 70% of 159 cells on four coverslips (Fig. 2B; Table 2).

cGMP levels in the pineal gland appear to be regulated by NE and VIP acting through an NO-dependent mechanism; accordingly, NO generators elevate pineal cGMP levels (29–31). In this study we found that the NO-generating agent SNAP (1 mM) increased $[Ca^{2+}]_i$ in 83% of 267 cells on 10 coverslips (Fig. 3; Table 2). We also tested the effect of three different concentrations (10 μM, 100 μM, and 1 mM) of SNAP on cells on one coverslip. All three concentrations were effective in eliciting a $[Ca^{2+}]_i$ response. The peak responses ($\Delta[Ca^{2+}]_i$) were 30.8 ± 3.4, 37.4 ± 3.1, and 82.5 ± 5.9 nM (mean ± standard error, $n = 36$) for 10 μM, 100 μM, and 1 mM SNAP, respectively, and the integrated areas under the peaks were 1.4 ± 0.2, 1.8 ± 0.2, and 6.0 ± 0.4 nM·sec, respectively. Similar results were obtained with another NO donor, 2,2-diethyl-1-nitroxyhydrazine (1 mM; 92 cells on three coverslips). This NO donor caused a peak response ($\Delta[Ca^{2+}]_i$) of 110.3 ± 0.8 nM (mean ± standard error) and an integrated response of 2.6 ± 0.2 nM·sec.

Comparison of the responses to SNAP and 8-Br-cGMP revealed that the response to the former was more sustained, as judged by the response at 90 sec (Tables 2 and 3). At 90 sec after the start of treatment, the response to 8-Br-cGMP was 17.8 ± 0.8% of the peak (162 cells from 12 coverslips), whereas the response to SNAP at the same time point was 49.6 ± 1.7% of the peak (261 cells from nine coverslips). This difference was statistically significant ($p < 0.001$).

Role of extracellular Ca^{2+}. It is known that agonist-induced $[Ca^{2+}]_i$ signals depend upon release of Ca^{2+} from intracellular stores, an increased influx of Ca^{2+} across the plasma membrane, or a combination of these. To determine the relative importance of these mechanisms in the $[Ca^{2+}]_i$ responses of pinealocytes to VIP and NE, the $[Ca^{2+}]_i$ responses of individual cells were determined in low-Ca^{2+} ($[Ca^{2+}]_o = 5$ μM) and normal-Ca^{2+} ($[Ca^{2+}]_o = 1.5$ mM) media. In normal-Ca^{2+} medium, both VIP and NE elevated $[Ca^{2+}]_i$ (Fig. 4A), as described above. In low-Ca^{2+} medium, however, the VIP-induced increase in $[Ca^{2+}]_i$ was nearly completely abolished, whereas only the plateau component of the NE-induced response was eliminated (Figs. 4B and 5A).

To quantitatively compare the response profiles, cells were initially challenged with either VIP or NE in low-Ca^{2+} medium, followed by stimulation in normal-Ca^{2+} medium (Fig. 5). In medium containing 5 μM Ca^{2+}, the response to VIP treatment was absent and the initial response to NE was present. However, after the $[Ca^{2+}]_o$ was increased to 1.5 mM, VIP treatment caused an increase in $[Ca^{2+}]_i$ (Fig. 5B) and NE treatment caused an increase in $[Ca^{2+}]_i$ that included both transient and sustained plateau phases. The VIP-induced peak $[Ca^{2+}]_i$ response was inhibited by 85% in the low-Ca^{2+} medium (Table 3). In contrast, the initial NE-induced peak response was reduced by only 16% (Table 3), confirming the aforementioned indications that the peak component of the $[Ca^{2+}]_i$ response to VIP is nearly entirely dependent upon $[Ca^{2+}]_o$ and that the peak component of the $[Ca^{2+}]_i$ response to NE is primarily dependent upon mobilization of stored Ca^{2+}, in agreement with published results (14). The NE-induced $[Ca^{2+}]_i$ response after 90 sec of treatment was 13% of the peak response in the low-Ca^{2+} medium, compared with 51% in normal medium (Table 3), in agreement with reports in the literature indicating that the plateau component of the response is strongly dependent on Ca^{2+} influx (17, 20). This change in the shape of the NE-induced $[Ca^{2+}]_i$ response in low-Ca^{2+} medium was reflected as a large reduction (64%) in the integrated $[Ca^{2+}]_i$ response (Table 3).

Similar experiments were performed in which cells were treated sequentially with cGMP protagonists in normal-Ca^{2+} medium and then low-Ca^{2+} medium. The $[Ca^{2+}]_i$ responses to 8-Br-cGMP and SNAP were reduced 90% and 83%, respectively, in low-Ca^{2+} medium (Fig. 6; Table 3).

Effects of *l-cis*-diltiazem and other channel blockers. The experiments presented above point to Ca^{2+} influx as a dominant mechanism driving the $[Ca^{2+}]_i$ response to VIP or cGMP protagonists. The effect of VIP was tested in the presence of three known blockers of voltage-dependent Ca^{2+} channels in a mixture, i.e., D-600 (1 μM), ω-conotoxin (0.1 μM), and the dihydropyridine nicardipine (1 and 10 μM). None prevented the VIP-mediated $[Ca^{2+}]_i$ increase but all were able to abolish or inhibit the increase in $[Ca^{2+}]_i$ evoked by treatment with high extracellular K^+ levels or veratridine (data not shown).

l-cis-Diltiazem, a blocker of rod CNG cation channels (32), was also tested (Fig. 7; Table 4). The concentration selected (25 μM) was typically used to selectively inhibit these cation channels in previously published studies (33–35). Cells were challenged sequentially with VIP (100 nM), 8-Br-cGMP (1 mM), and NE (1 μM). In the absence of *l-cis*-diltiazem (three coverslips) (Fig. 7A), $[Ca^{2+}]_i$ was increased by VIP in 69% of the cells, by 8-Br-cGMP in 47%, and by NE in 93%, in general agreement with the results described above. In a separate set of experiments, cells were treated with *l-cis*-diltiazem for 5 min and then with agonists in the presence of the blocker. In the presence of *l-cis*-diltiazem (two coverslips) (Fig. 7B), the peak $[Ca^{2+}]_i$ responses to VIP (100 nM) or 8-Br-cGMP were significantly reduced, by 87 and 82%, respectively ($p < 0.001$) (Table 4). In contrast, the peak $[Ca^{2+}]_i$ response to NE was reduced by only 24% ($p < 0.7$). This indicates that the peak $[Ca^{2+}]_i$ responses to VIP and 8-Br-cGMP are strongly dependent upon a *l-cis*-diltiazem-sensitive process and those of NE are markedly less dependent. Analysis of the responses detected at 90 sec and of the integrated responses supports this interpretation (Table 4). For example, *l-cis*-diltiazem significantly reduced the integrated response to VIP by 50% and that to 8-Br-cGMP by ~85% ($p < 0.005$ and 0.001, respectively) but did not significantly reduce the integrated response to NE ($p < 0.8$). In four different trials on separate coverslips, 25 μM *d-cis*-diltiazem was found to be ineffective in inhibiting the VIP-induced $[Ca^{2+}]_i$ response. For these reasons we believe that our results are consistent with the interpretation that CNG cation channels may be involved in the VIP-induced $[Ca^{2+}]_i$ response in rat pineal cells.

Evidence for the presence of mRNA encoding the rod-type CNG cation channel in pinealocytes. Our data indicate that a *l-cis*-diltiazem-sensitive mechanism mediates

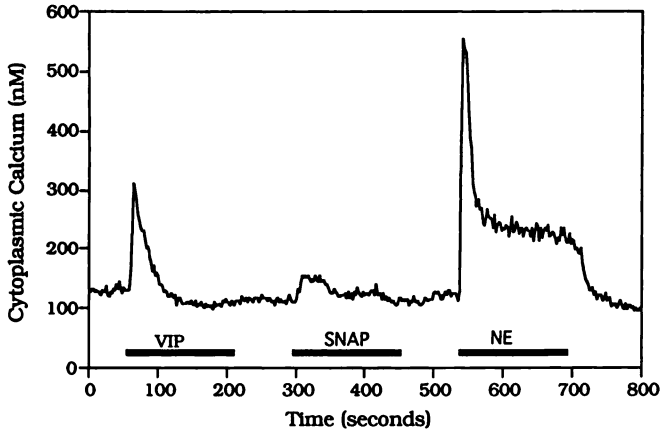

Fig. 3. Effect of SNAP on $[Ca^{2+}]_i$ in pinealocytes. Pinealocytes were plated as described in Materials and Methods, loaded with fura-2/AM, and perfused at the rate of 1.5 ml/min at 37° for at least 300 sec before the beginning of the recording (time 0). SNAP (1 mM) treatment was initiated as indicated (*bars*). A quantitative summary of experiments represented here appears in Table 2.

the effects of VIP and 8-Br-cGMP in the pineal gland, suggesting that a rod-type CNG cation channel is present in this tissue. To examine this hypothesis, RT-PCR analysis was conducted. mRNA was extracted from the rat pineal gland, retina, and cerebellum. A single abundant product was generated with cDNA from pineal gland and retina (Fig. 8). The size of the product (~650 bp) agrees well with that predicted from the published sequence for the human rod-type CNG cation channel (684 bp) (31). Using identical conditions, it was not possible to generate a similar product using cDNA prepared from rat cerebellum. Serial dilution indicated that the mRNA encoding the CNG cation channel is manyfold more abundant in the retina than in the pineal gland. Quantitative PCR analysis will be required, however, to clearly establish the relative abundance of the mRNA encoding this channel in these tissues. Sequence analysis of the pineal and retinal RT-PCR products (Fig. 8) indicated that they are 92% identical to the corresponding region of the mouse CNG channel sequence (36), confirming that the CNG channel is expressed in the rat pineal gland. While this manuscript was under review, the presence of mRNA encoding retinal rod-type CNG cation channels in the bovine pineal gland was reported (37).

Discussion

The results presented here are of special importance for three reasons. First, they provide the first indication that VIP elevates $[Ca^{2+}]_i$ in pinealocytes, as is true in anterior pituitary cells, diencephalic neurons, and hippocampal neurons in culture (16–19, 28). The observation that a $[Ca^{2+}]_i$ signal is induced in most pinealocytes by VIP and NE indicates that essentially all pinealocytes are sensitive to both agonists and that distinct VIP-sensitive and NE-sensitive subtypes do not exist. This is consistent with the observation that the effects of VIP on cyclic nucleotide levels in pinealocytes in suspension culture are potentiated by α-adrenergic stimulation (7, 38), which probably reflects interactions distal to receptor activation within individual cells (6).

Second, the mechanism through which VIP increases

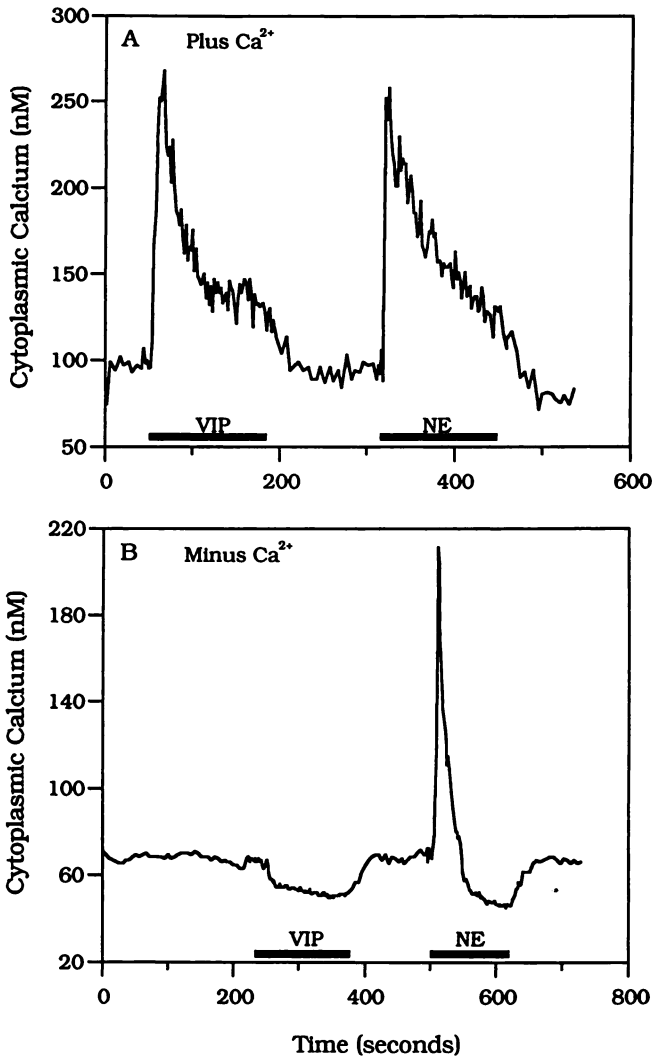

Fig. 4. Role of extracellular Ca^{2+} in the effect of NE and VIP on $[Ca^{2+}]_i$. Pinealocytes were plated as described in Materials and Methods, loaded with fura-2/AM, perfused at the rate of 1.5 ml/min at 37° for 300 sec before the beginning of the recording time (time 0). *A*, normal medium; *B*, Ca^{2+}-depleted medium ($[Ca^{2+}]_o$ = 5 μM). NE (1 μM) or VIP (100 nM) treatment was initiated as indicated (*bars*). Similar results were obtained with 52 cells on three coverslips.

$[Ca^{2+}]_i$ in pinealocytes appears to be novel. In several other cellular systems, it has been found that cAMP mediates the effects of VIP on $[Ca^{2+}]_i$ (16, 17, 28, 39). However, cAMP does not appear to play a similar role in pinealocytes, based on the observations that cAMP protagonists, including DB-cAMP and forskolin, do not increase $[Ca^{2+}]_i$.

Rather, cGMP appears to mediate the effects of VIP on pinealocyte $[Ca^{2+}]_i$. The evidence from pineal studies is that 1) VIP elevates cGMP accumulation >10-fold (38); 2) the cGMP analogs 8-Br-cGMP and DB-cGMP elevate $[Ca^{2+}]_i$; 3) SNAP, a compound that elevates cGMP through generation of NO, elevates $[Ca^{2+}]_i$; 4) VIP, 8-Br-cGMP, and SNAP elevate $[Ca^{2+}]_i$ through a mechanism that requires extracellular Ca^{2+}; 5) the effects of VIP and 8-Br-cGMP are blocked by *l-cis*-diltiazem, which is known to block the rod-type CNG cation channel; and 6) RT-PCR analysis indicates that the rod-type CNG cation channel is expressed in the pineal gland. Accordingly, it seems reasonable to suspect that a

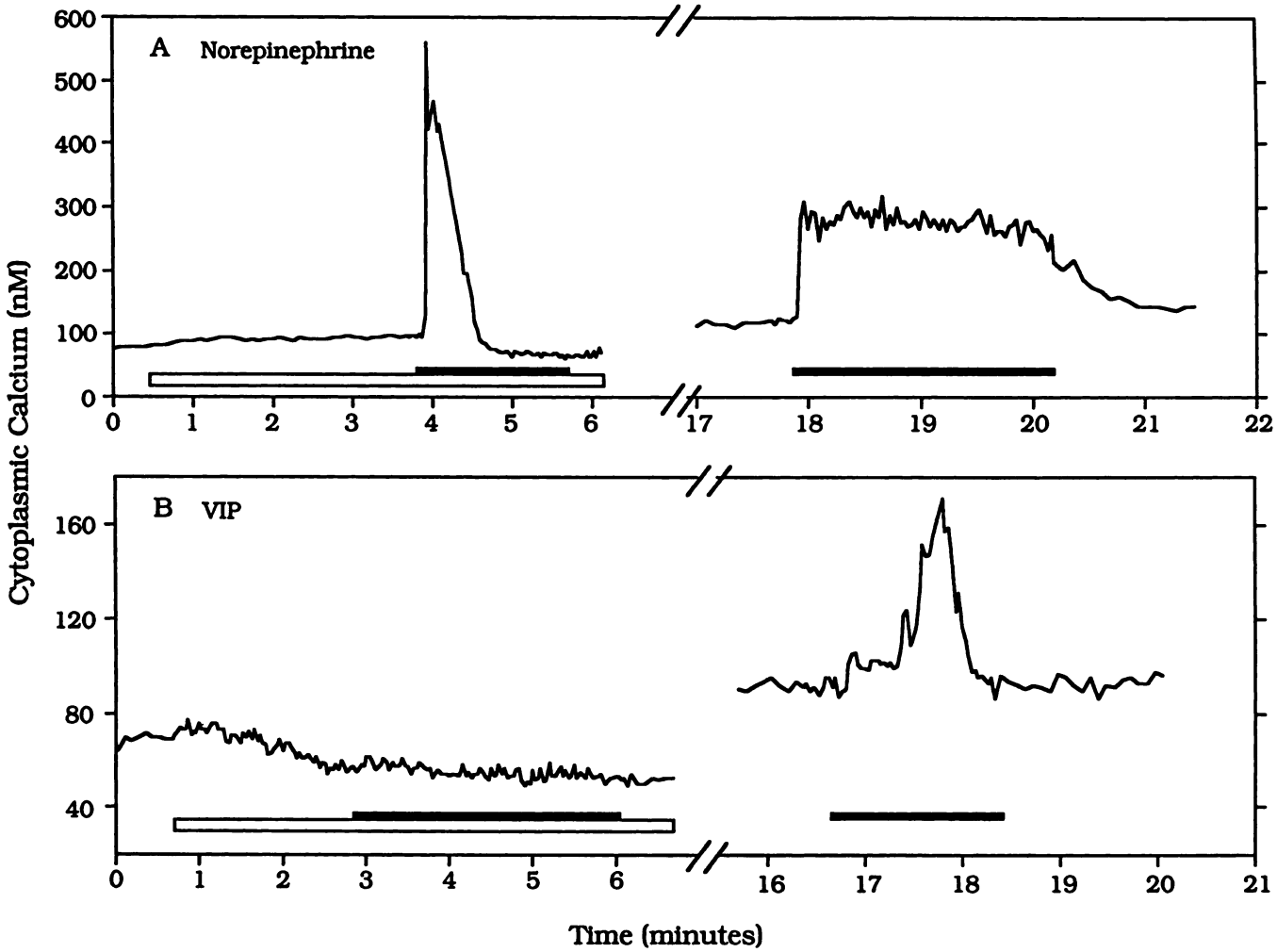

Fig. 5. Comparison of the effects of VIP and NE in normal-Ca^{2+} and low-Ca^{2+} media. Pinealocytes were plated as described in Materials and Methods, loaded with fura-2/AM, and perfused at the rate of 1.5 ml/min at 37° for at least 300 sec before the beginning of the recording (time 0). Cells were initially perfused (*white bars*) with low-Ca^{2+} medium ($[Ca^{2+}]_o$ = 5 μM) and then perfused with normal-Ca^{2+} medium ($[Ca^{2+}]_o$ = 1.5 mM). The duration of treatment (100 nM VIP or 1 μM NE) is indicated (*black bars*). A quantitative summary of experiments represented here appears in Table 3.

VIP/cGMP/$[Ca^{2+}]_i$ regulatory mechanism exists in the pineal gland and that a rod-type CNG cation channel mediates the effects of cGMP.

Although our studies point to the probable existence of this channel in mammalian pinealocytes, it should be emphasized that appropriate electrophysiological, biochemical, and molecular analyses are required to fully characterize this channel and to determine whether it is identical to the channel found in the retina or elsewhere (40). However, the expression of the retinal CNG channel in mammalian pinealocytes would be consistent with electrophysiological evidence that this channel occurs in avian pinealocytes (41). It would also be consistent with the expression of a number of other retinal phototransduction-related proteins, including S-antigen (arrestin), Met-Glu-Lys-Ala (phosducin), and opsin kinase (42), in mammalian pineal gland.

A third reason the results of the studies presented here are of special importance is that they establish a role for cGMP in mammalian pinealocytes. Before these investigations, cGMP was not thought to play a role in pinealocyte cell physiology, although cGMP levels were known to be regulated by NE and VIP (6, 38). The evidence indicating that cGMP influences $[Ca^{2+}]_i$ gives this second messenger a role in pineal cell physiology.

In addition to the issues discussed above, several other aspects of our investigation deserve further comment, including comparison of the VIP- and NE-evoked $[Ca^{2+}]_i$ signals in pinealocytes and differences in the $[Ca^{2+}]_i$ responses to 8-Br-cGMP and SNAP. These are discussed below.

Comparison of the $[Ca^{2+}]_i$ responses to VIP and NE observed in our studies reveals some marked differences in the peak and plateau components. Typically, the VIP response has a smaller peak amplitude and is short lived, with relatively little or no plateau response. The peak response to NE, however, is typically of greater amplitude and the plateau phase is sustained and pronounced. The results of our studies and of others (11, 14) indicate that these agonists cause an increase in $[Ca^{2+}]_i$ through different mechanisms, which probably explains the differences in the patterns of these responses.

It appears that the primary mechanism involved in the effects of VIP is an ionotropic mechanism, i.e., cGMP activation of a rod-type CNG channel, and that this response is relatively transient. In contrast, this mechanism does not

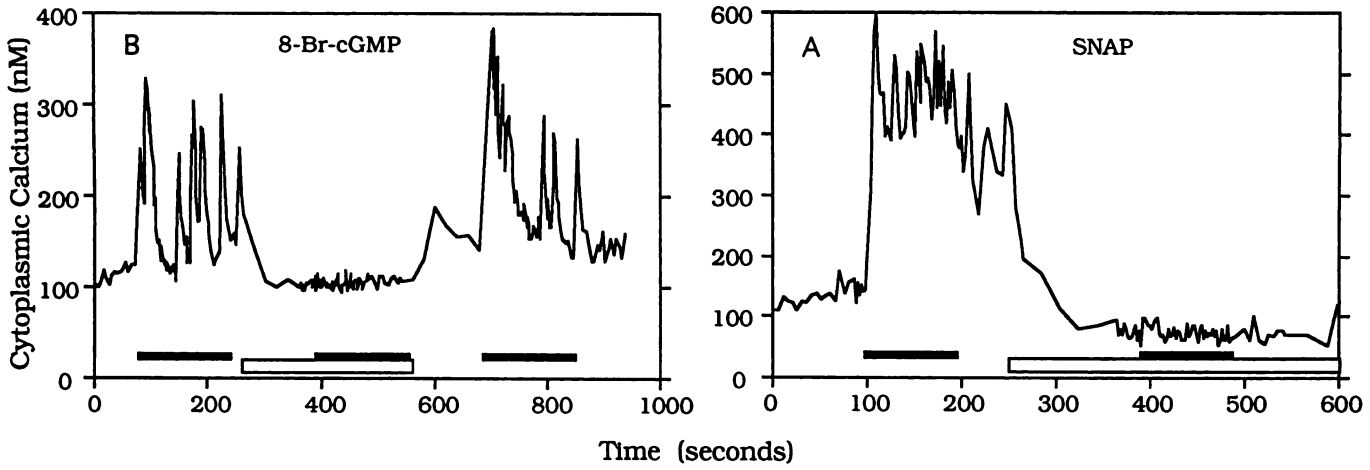

Fig. 6. Role of extracellular Ca^{2+} in the effect of 8-Br-cGMP and SNAP. Pinealocytes were plated as described in Materials and Methods, loaded with fura-2/AM, and perfused at the rate of 1.5 ml/min at 37° for 300 sec before the beginning of the recording (time 0). A, Effect of SNAP. Cells were treated with 1 mM SNAP (*first black bar*), the medium was changed to a low-Ca^{2+} medium ($[Ca^{2+}]_o$ = 5 μM) (*white bar*), and the treatment was repeated (*second black bar*). B, Effect of 8-Br-cGMP treatment. Cells were treated with 1 mM 8-Br-cGMP (*first black bar*), the medium was changed to a low-Ca^{2+} medium ($[Ca^{2+}]_o$ = 5 μM) (*white bar*), and the treatment was repeated (*second black bar*). Cells were then rechallenged with 8-Br-cGMP in normal medium (*third black bar*). A quantitative summary of experiments represented here appears in Table 3.

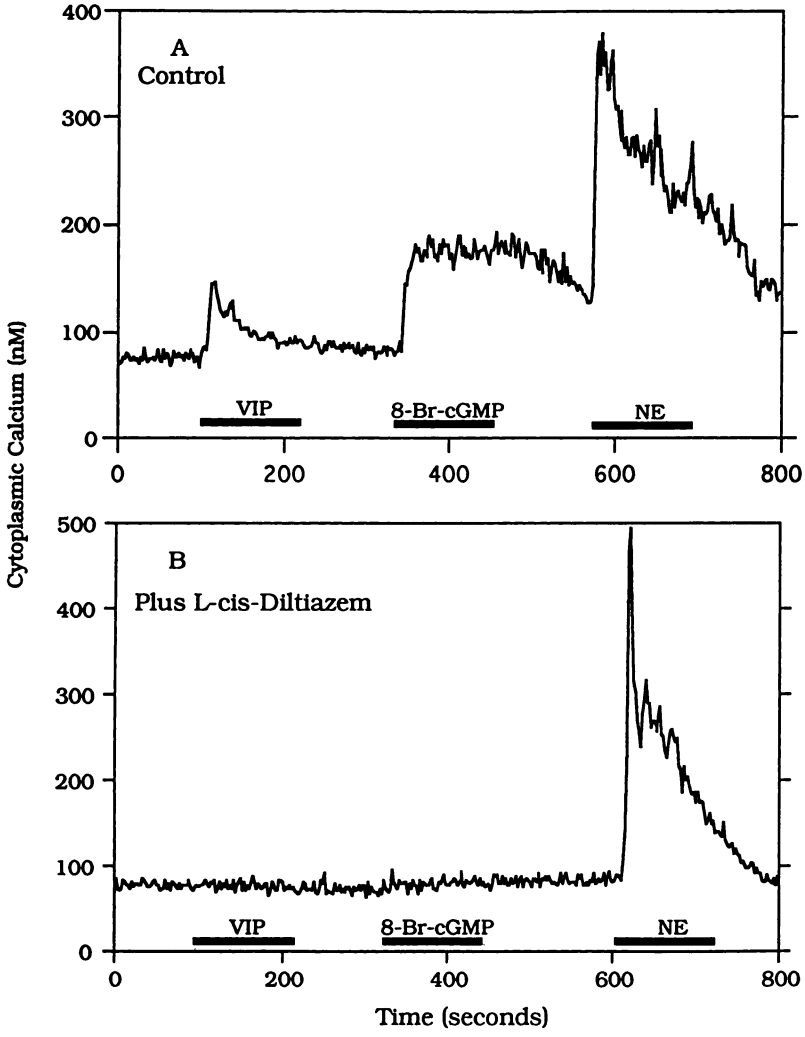

Fig. 7. Effects of VIP, 8-Br-cGMP, and NE on $[Ca^{2+}]_i$ in *l-cis*-diltiazem-treated cells. Pinealocytes were plated as described in Materials and Methods, loaded with fura-2/AM, and perfused at the rate of 1.5 ml/min at 37° for at least 300 sec before the beginning of the recording (time 0). A, Responses in the absence of *l-cis*-diltiazem. Cells were treated sequentially with 100 nM VIP, 1 mM 8-Br-cGMP, and 1 μM NE. B, Responses in diltiazem-treated cells. Cells were perfused for 120 sec with normal medium and then for 180 sec with *l-cis*-diltiazem (25 μM) before the beginning of the experiment. A quantitative summary of experiments represented here appears in Table 4.

appear to play a major role in the peak component of the $[Ca^{2+}]_i$ response to NE, because it is only weakly reduced in low-Ca^{2+} medium and is not strongly antagonized by *l-cis*-diltiazem. Rather, the dominant mechanism generating the peak component of the $[Ca^{2+}]_i$ response to NE does not seem to involve extracellular Ca^{2+} and is primarily dependent

TABLE 4

Effect of *l-cis*-diltiazem (25 μM) on $[Ca^{2+}]_i$ responses to selected agents

Cells were treated with *l-cis*-diltiazem for 5 min and then with the agents listed, in the presence of *l-cis*-diltiazem. This summarizes the results of a series of experiments, examples of which appear in Fig. 7. Data are presented as the mean ± standard error. Response data were all obtained from the same preparations of cells on two coverslips. *n*, number of cells analyzed.

Agent	*l-cis*-Diltiazem	$[Ca^{2+}]_i$ response[a]		Integrated response[b]	*n*
		Peak[c]	90 sec[d]		
		nM		μM·sec	
VIP (0.1 μM)	−	153 ± 5.50	19.8 ± 6.00	10.2 ± 0.24	94
	+	20 ± 4.00 (87%)	1.8 ± 1.70	5.1 ± 0.24	37
NE (1 μM)	−	243 ± 13.1	133 ± 9.70	27.6 ± 1.70	94
	+	186 ± 20.0 (24%)	82 ± 12.0	24.1 ± 2.00	37
8-Br-cGMP (1 mM)	−	100 ± 1.70	10 ± 2.00	7.0 ± 0.40	94
	+	18 ± 3.00 (82%)	6 ± 2.00	1.1 ± 0.09	37

[a] Response values have had pretreatment values subtracted on a cell-by-cell basis.
[b] The integrated response reflects the response during the first 3 min of treatment.
[c] In all cases peak responses occurred during the first 10 sec of treatment. Numbers in parentheses are percentage reduction in the response, compared with the response when no drug was present.
[d] Values are $[Ca^{2+}]_i$ at 90 sec after initiation of treatment, which provides a measure of the response during the plateau phase.

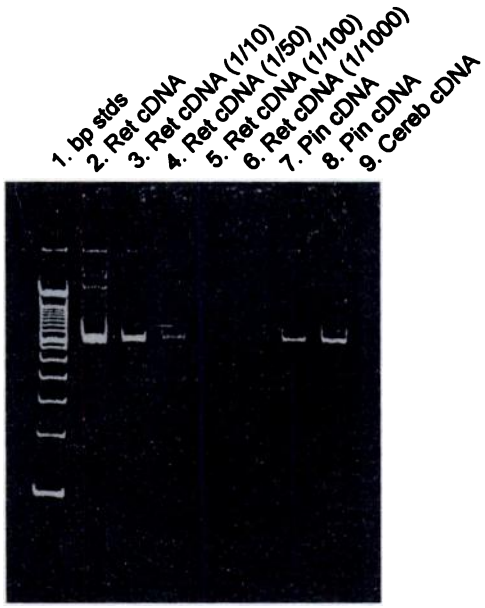

Fig. 8. RT-PCR analysis of the presence of the rod-type CNG cation channel in rat pineal gland and retina. mRNA was extracted from rat retina and pineal tissue, cDNA was synthesized, and PCR was performed as described in Materials and Methods. The prominent band migrated between the 600- and 700-bp standard markers, with an estimated size of approximately 650 bp. Signals were not generated if template was excluded or if one of the primers was excluded. Each lane contained a 5-μl sample, as follows: *lane 1*, standards; *lane 2*, retinal (*Ret*) cDNA; *lane 3*, retinal cDNA, diluted 1/10; *lane 4*, retinal cDNA, diluted 1/50; *lane 5*, retinal cDNA, diluted 1/100; *lane 6*, retinal cDNA, diluted 1/1000; *lane 7*, pineal (*Pin*) cDNA, batch 1; *lane 8*, pineal cDNA, batch 2; *lane 9*, cerebellum (*Cereb*) cDNA.

upon mobilization of stored Ca^{2+}. It seems likely that this reflects a metabotropic mechanism, i.e., α-adrenergic stimulation of inositol trisphosphate generation through activation of phospholipase C (43). The plateau component of the $[Ca^{2+}]_i$ response to NE appears to be dependent upon enhanced influx, based on findings described here and elsewhere (11, 14). This influx mechanism does not appear to be highly sensitive to *l-cis*-diltiazem, and it is not clear whether the enhanced influx is secondary to the metabotropic effect of NE or represents an independent ionotropic mechanism, or a combination of both.

The conclusion that NE elevates $[Ca^{2+}]_i$ through a metabotropic mechanism involving release of stored Ca^{2+} is not in total agreement with the conclusions of prior studies in which pinealocytes were studied in suspension (11). In those studies a rapid peak $[Ca^{2+}]_i$ response was not evident, although it was clear that NE caused a sustained elevation of $[Ca^{2+}]_i$. The failure to detect a rapid peak response in the earlier studies might reflect experimental differences, including the nature and concentration of Ca^{2+} dyes used, the temporal resolution of the detection system, and the fact that a population of cells was studied.

The functional significance of the smaller and transient $[Ca^{2+}]_i$ response to VIP might be that this is the basis of the smaller cAMP, NAT, and melatonin production responses induced by VIP, compared with NE. Another possibility is that the transient effects of VIP on $[Ca^{2+}]_i$ reflect a special action of VIP. Perhaps the release of VIP and the resulting transient elevation of $[Ca^{2+}]_i$ are not primarily related to melatonin production but, rather, are related to another function that does not require long term elevation of $[Ca^{2+}]_i$. For example, transient elevation of $[Ca^{2+}]_i$ might be sufficient to release stored molecules or to maintain expression of a gene.

Another interesting issue to consider is the basis of the differences in the patterns of the $[Ca^{2+}]_i$ responses to 8-Br-cGMP and SNAP (Tables 2 and 3). If both were acting exclusively through cGMP, then the patterns of the $[Ca^{2+}]_i$ responses might be similar. However, it appears from the limited observations made here that the $[Ca^{2+}]_i$ response to the NO generator SNAP was distinctly more sustained than the response to 8-Br-cGMP. Two hypothetical explanations for this can be considered. One is that NO elevates $[Ca^{2+}]_i$ through cGMP-dependent and cGMP-independent mechanisms. The cGMP-independent effects might produce a sustained increase in $[Ca^{2+}]_i$, perhaps through a mechanism similar to that in bovine pulmonary artery endothelial cells (44). Another explanation is that 1 mM 8-Br-cGMP treatment produced autoinhibition of the response and SNAP did not. It seems reasonable to suspect that this might occur, because NO stimulation of endogenous generation of cGMP might not elevate cGMP to levels that antagonize stimulation of the channel, whereas 1 mM 8-Br-cGMP might do so. In addition, the concentrations of SNAP used in this study greatly exceed

the doses that maximally stimulate soluble guanylyl cyclase and thus are expected to generate extremely high levels of NO in cells. Under these conditions, the potential exists for non-cGMP-mediated signaling to cause $[Ca^{2+}]_i$ increases. The fact that in cells treated with 1 mM SNAP the resting $[Ca^{2+}]_i$ returned to original levels after removal of SNAP and the cells retained their responsiveness to NE suggests that the observed response is not due to overt toxicity of SNAP. In addition, we found that lower concentrations of SNAP were also effective in eliciting the $[Ca^{2+}]_i$ response and that the structurally distinct NO generator 2,2-diethyl-1-nitroxyhydrazine also elevated $[Ca^{2+}]_i$.

These studies emphasize the value of pinealocytes as a model system for analysis of the molecular effects of VIP. It will be of interest to determine whether cells in other neural structures share the VIP/cGMP/$[Ca^{2+}]_i$ transduction system suggested by these studies or whether it is unique to pinealocytes.

Acknowledgments

We would like to express our appreciation to Dr. King Wai Yau (Johns Hopkins School of Medicine) for his generous gift of *l-cis*-diltiazem, to Dr. Tambra Duna (National Cancer Institute) for his generous gift of *l*-2,2-diethyl-1-nitroxyhydrazine, and to Dr. Patrick Roseboom (National Institute of Child Health and Human Development) for assistance in designing primers for RT-PCR analysis. We thank Mr. Chanh Lienvongkot for help in writing macros for data analysis.

References

1. Kaku, K., Y. Inoue, A. Matsutani, M. Okubo, K. Hatao, T. Kaneko, and N. Yanaihara. Receptors for vasoactive intestinal polypeptide on rat dispersed pineal cells. *Biomed. Res.* **4**:321–328 (1983).
2. Piszczkiewicz, S., and R. E. Zigmond. Is the vasoactive intestinal peptide-like immunoreactivity in the rat pineal gland present in fibers originating in the superior cervical ganglion? *Brain Res.* **593**:327–331 (1992).
3. Kaneko, T., P. Y. Cheng, H. Oka, T. Oda, N. Yahaihara, and C. Yanaihara. Vasoactive intestinal polypeptide stimulates adenylate cyclase and serotonin *N*-acetyltransferase activities in rat pineal *in vitro*. *Biomed. Res.* **1**:84–87 (1980).
4. Yuwiler, A. Vasoactive intestinal peptide stimulation of pineal serotonin *N*-acetyltransferase (EC 2.3.1.5) activity: general characteristics. *J. Neurochem.* **41**:146–153 (1983).
5. Yuwiler, A. Light and agonists alter pineal *N*-acetyltransferase (EC 2.3.1.5) induction by vasoactive intestinal polypeptide. *Science (Washington D. C.)* **220**:1082–1083 (1983).
6. Chik, C., A. Ho, and D. C. Klein. α_1-Adrenergic potentiation of vasoactive intestinal peptide stimulation of rat pinealocyte adenosine 3′,5′-monophosphate and guanosine 3′,5′-monophosphate: evidence for a role of calcium and protein kinase C. *Endocrinology* **122**:702–708 (1988).
7. Chik, C., A. Ho, and D. C. Klein. Dual receptor regulation of cyclic nucleotides: α-adrenergic potentiation of vasoactive intestinal peptide stimulation of pinealocyte adenosine 3′,5′-monophosphate. *Endocrinology* **122**: 1646–1651 1988).
8. Klein, D. C. Photoneural regulation of the mammalian pineal gland. *Ciba Found. Symp.* **117**:38–56 (1986).
9. Klein, D. C., D. Sugden, and J. L. Weller. Postsynaptic α_1-adrenergic receptors potentiate the β-adrenergic stimulation of pineal serotonin *N*-acetyltransferase. *Proc. Natl. Acad. Sci. USA* **80**:599–603 (1983).
10. Sugden, L., D. Sugden, and D. C. Klein. Essential role of calcium influx in the adrenergic regulation of cAMP and cGMP in rat pinealocytes. *J. Biol. Chem.* **261**:11608–11612 (1986).
11. Sugden, L., D. Sugden, and D. C. Klein. α_1-Adrenoceptor activation elevates cytosolic calcium in rat pinealocytes by increasing net influx. *J. Biol. Chem.* **262**:741–745 (1987).
12. Yuwiler, A. Synergistic action of postsynaptic *alpha*-adrenergic receptor stimulation on vasoactive intestinal polypeptide-induced increase in pineal *N*-acetyltransferase activity. *J. Neurochem.* **49**:806–811 (1987).
13. Schaad, N. C., A. Parfitt, H.-W. Korf, A. R. Schaffner, J. T. Russell, and D. C. Klein. Single cell analysis and biochemical characterization of pinealocytes immobilized with novel attachment peptide preparation. *Brain Res.* **614**:251–256 (1993).
14. Saez, J., A. P. Moreno, and D. C. Spray. Norepinephrine induced Ca^{2+} release from intracellular stores in rat pinealocytes. *J. Pineal Res.* **16**: 57–64 (1994).
15. Ceña, V., J. I. Halperin, S. Yeandle, and D. C. Klein. Norepinephrine stimulates potassium efflux from pinealocytes: evidence for involvement of biochemical "AND" gate operated by calcium and adenosine 3′,5′-monophosphate. *Endocrinology* **128**:559–569 (1991).
16. Luini, A., D. Lewis, S. Guild, D. Corda, and J. Axelrod. Hormone secretagogues increase cytosolic calcium by increasing cAMP in corticotropin-secreting cells. *Proc. Natl. Acad. Sci. USA* **82**:8034–8038 (1985).
17. Kase, H., M. Wakui, and O. H. Petersen. Stimulatory and inhibitory actions of VIP and cyclic AMP on cytoplasmic calcium signal generation in pancreatic acinar cells. *Pfluegers Arch.* **419**:668–670 (1991).
18. Tatsuno, I., T. Yada, S. Vigh, H. Hidaka, and A. Arimura. Pituitary adenylate cyclase activating polypeptide and vasoactive intestinal peptide increase cytosolic free calcium concentration in cultured rat hippocampal neurons. *Endocrinology* **131**:73–81 (1992).
19. Fatatis, A., L. A. Holtzclaw, R. Avidor, D. E. Brenneman, and J. T. Russell. Vasoactive intestinal peptide increases intracellular calcium in astroglia: synergism with *alpha*-adrenergic receptors. *Proc. Natl. Acad. Sci. USA* **91**:2036–2040 (1994).
20. Fatatis, A., and J. T. Russell. Spontaneous changes in intracellular calcium concentration in type 1 astrocytes from rat cerebral cortex in primary culture. *Glia* **5**:95–104 (1992).
21. Yagodin, S. V., L. Holtzclaw, C. A. Sheppard, and J. T. Russell. Non-linear propagation of agonist-induced cytoplasmic calcium waves in single astrocytes. *J. Neurobiol.* **25**:265–280 (1994).
22. Grynkiewicz, G., M. Poenie, and R. Y. Tsien. A new generation of Ca^{2+} indicators with greatly improved fluorescence properties. *J. Biol. Chem.* **260**:3440–3450 (1985).
23. Williams, D. A., K E. Fogarty, R. Y. Tsien, and F. S. Fay. Calcium gradients in single smooth muscle cells revealed by the digital imaging microscope using fura-2. *Nature (Lond.)* **318**:558–561 (1985).
24. Chomczynski, P., and N. Sacchi. Single-step method of RNA isolation by acid guanidinium thiocyanate phenol-chloroform extraction. *Anal. Biochem.* **162**:156–159 (1987).
25. Dhallan, R. S., J. P. Macke, R. L. Eddy, T. B. Shows, R. R. Reed, K. W. Yau, and J. Nathans. Human rod photoreceptor cGMP-gated channel: amino acid sequence, gene structure, and functional expression. *J. Neurosci.* **12**:3248–3256 (1992).
26. Devereux, J., P. Haeberli, and O. Smithies. A comprehensive set of sequence analysis programs for VAX and CONVEX systems. *Nucleic Acids Res.* **12**:387–395 (1984).
27. Winer, B. J. *Statistical Principles in Experimental Design*. McGraw Hill, New York (1971).
28. Bjoro, T., B. C. Ostberg, O. Sand, J. Gordeladze, J.-G. Iversen, P. A. Torjesen, K. M. Ggautvik, and E. Haug. Vasoactive intestinal peptide and peptide with amino-terminal histidine and carboxyl-terminal isoleucine increase prolactin secretion in cultured rat pituitary cell GH_4C_1 via a cyclic AMP-dependent mechanism which involves transient elevation of intracellular calcium. *Mol. Cell. Endocrinol.* **49**:119–128 (1987).
29. Spessert, R. Vasoactive intestinal peptide stimulation of cyclic guanosine monophosphate formation: further evidence for a role of nitric oxide synthase and cytosolic guanylate cyclase in rat pinealocytes. *Endocrinology* **132**:2513–2517 (1993).
30. Spessert, R., E. Layes, and L. Vollrath. Adrenergic stimulation of cGMP formation requires NO-dependent activation of cytosolic guanylate cyclase in rat pinealocytes. *J. Neurochem.* **61**:138–143 (1993).
31. Lin, A. M.-Y., N. C. Schaad, P. E. Schulz, S. L. Coon, and D. C. Klein. Pineal nitric oxide synthase: characteristics, adrenergic regulation and function. *Brain Res.* **651**:160–168 (1994).
32. Koch, K. W., and U. B. Kaupp. Cyclic GMP directly regulates a cation conductance in membranes of bovine rods by a cooperative mechanism. *J. Biol. Chem.* **260**:6788–6800 (1985).
33. Cook, N. J., W. Hanke, and U. B. Kaupp. Identification, purification, and reconstitution of the cyclic GMP-dependent channel from rod photoreceptors. *Proc. Natl. Acad. Sci. USA* **84**:585–589 (1987).
34. Pearce, L. B., R. D. Calhoon, P. R. Burns, A. Vincent, and S. M. Goldin. Two functionally distinct forms of guanosine cyclic 3′,5′-phosphate stimulated cation channels in a bovine rod photoreceptor disk preparation. *Biochemistry* **27**:4396–4406 (1988).
35. Kaupp, U. B., T. Niidome, T. Tanabe, S. Terada, W. Bomigk, W. Stuhmer, N. J. Cook, K. Kangawa, H. Matsuo, T. Hirose, T. Miyata, and S. Numa. Primary structure and functional expression from complementary DNA of the rod photoreceptor cyclic GMP-gated channel. *Nature (Lond.)* **342**:762–766 (1989).
36. Baehr, W., J. J. Wasmuth, R. L. Hurwitz, M. F. Seldin, T. A. Howard, M. R. Altherr, A. K. Lee, and S. J. Pittler. Primary structure and chromosomal localization of human and mouse rod photoreceptor cGMP-gated cation channel. *J. Biol. Chem.* **267**:6257–6262 (1994).
37. Distler, M., M. Biel, V. Flockerzi, and F. Hofmann. Expression of cyclic nucleotide-gated cation channels in non-sensory tissues and cells. *Neuropharmacology* **33**:1275–1282 (1994).
38. Chik, C., A. Ho, and D. C. Klein. Transmembrane receptor cross-talk: concurrent VIP and α_1-adrenergic activation rapidly elevates pinealocyte cGMP >100-fold. *Biochem. Biophys. Res. Commun.* **146**:1478–1484 (1987).

39. Quick, M., L. L. Iversen, and S. R. Bloom. Effect of vasoactive intestinal peptide (VIP) and other peptides on cAMP accumulation in rat brain. *Biochem. Pharmacol.* **27**:2209–2213 (1978).
40. Weyand, I., M. Godde, S. Frings, J. Weiner, F. Muller, W. Altenhofen, H. Hatt, and U. B. Kaupp. Cloning and functional expression of a cyclic nucleotide-gated channel from mammalian sperm. *Nature (Lond.)* **368**: 859–863 (1994).
41. Dryer, S. E., and D. Henderson. A cyclic GMP-activated channel in dissociated cells of the chick pineal gland. *Nature (Lond.)* **353**:756–758 (1991).
42. O'Brien, P. J., and D. C. Klein, eds. *Pineal and Retinal Relationships*. Academic Press, London (1986).
43. Ho, A. K., C. L. Chik, and D. C. Klein. Permissive role of calcium in α-adrenergic stimulation of pineal phosphatidylinositol phosphodiesterase (phospholipase C) activity. *J. Pineal Res.* **5**:553–564 (1988).
44. Inazu, M., H. Zhang, and E. E. Daniel. LP-805, a releaser of endothelium-derived nitric oxide, activates an endothelial calcium-permeable non-specific cation channel. *Life Sci.* **53**:315–320 (1993).

Send reprint requests to: James T. Russell, Building 49, Room 5A78, National Institutes of Health, Bethesda, MD 20892.